De novo bone formation underneath the sinus membrane supported by a bone patch: a pilot experiment in rabbit sinus model

So-Ra Yoon

Department of Dentistry

The Graduate School, Yonsei University

De novo bone formation underneath the sinus membrane supported by a bone patch: a pilot experiment in rabbit sinus model

Directed by Professor Ui-Won Jung

The Doctoral Dissertion
submitted to the Department of Dentistry,
the Graduate school of Yonsei University
in partial fulfillment of the requirements for the degree of
Ph.D. in Dental Science

So-Ra Yoon

June 2017

연세대학교
YONSEI UNIVERSITY

This certifies that the Doctoral Dissertation
of So-Ra Yoon is approved.

Thesis Supervisor : Ui-Won Jung

Seong-Ho Choi

Won-Gyun Chung

Sung-Tae Kim

Jung-Seok Lee

The Graduate School

Yonsei University

June 2017

감사의 글

배우고 때때로 익히면 또한 기쁘지 아니한가(學而時習之不亦說乎). <논어>의 첫 구절입니다. 흔한 말이지만 감사의 글은 꼭 이렇게 시작하고 싶었습니다. 저에게 연구자의 길을 걷는 것은 학문적 탐구의 즐거움을 깨닫는 과정이었기 때문입니다. 물론 가끔 흔들릴 때도 있었고, 힘들어 포기하고 싶을 때도 있었습니다. 그러나 탐구와 배움의 즐거움을 알아 버렸기에 이렇게 모든 과정을 마칠 수 있었습니다.

무엇보다 부족한 저에게 끊임없는 탐구 정신과 호기심을 일깨워주신 정의원 교수님께 진심으로 감사의 말씀 드립니다. 감사의 마음을 어떻게 글로 다 표현할지 모르겠습니다. 교수님을 통해 진정한 학자란 무엇인지 깨달을 수 있었습니다. 교수님의 가르침을 본받아 참된 연구자의 길을 계속 걷겠습니다. 또한 언제나 조언을 아끼지 않으신 최성호 교수님과 늘 격려해주신 정원균 교수님께 깊이 감사드립니다. 바쁘신 와중에도 심사를 맡아주시고 연구 방향을 제시해주신 김성태 교수님과 이중석 교수님께도 감사의 말씀 드립니다. 그 외에도 연구에 많은 도움을 주셨던 연구원, 수련의 선생님들께 진심으로 감사드립니다. 힘들고 지칠 때마다 곁에서 응원해준 친구들 모두에게도 고마움을 전합니다.

마지막으로 따뜻한 응원과 격려해주신 이모, 이모부, 누리, 누림언니와 우리 오빠, 가족들에게 정말 감사드립니다. 늘 믿어주시며 사랑받는 막내딸로 키워주시고 버팀목이 되어주신 어머니 아버지, 늘 존경하고 사랑합니다.

2017 년 6 월

저자 씀

TABLE OF CONTENTS

LIST OF FIGURES

LIST OF TABLES

ABSTRACT

De novo bone formation underneath the sinus membrane supported by a bone patch: a pilot experiment in rabbit sinus model

So-Ra Yoon

Department of Dentistry

The Graduate School, Yonsei University

(Directed by Professor Ui-Won Jung, D.D.S., M.S.D., PhD.)

Purpose

The objectives of this study were to evaluate bone regeneration beneath a newly devised bone substitute combined with collagen membrane (called a bone patch) lying over a concomitantly placed mini-implant following sinus floor elevation, and verify its usefulness as a carrier system for recombinant human bone morphogenetic protein-2 (rhBMP-2) in rabbits.

Materials and Methods

The sinus floor elevation procedure was performed bilaterally in five rabbits. Either a plain bone patch (control group) or an rhBMP-2 loaded patch (experimental group)

was randomly placed beneath the elevated sinus membrane of both sinuses, where the mini-implants were concomitantly placed. Micro-computed tomographic and histologic analyses were performed at 4 weeks post-surgery.

Results

In micro-computed tomography, the median values of the total augmented volume and the mineralized bone volume were significantly higher in the experimental group than in the control group (161 vs. 122 mm^3 [P<0.01] and 48 vs. 42 mm3 [P<0.05], respectively). Histometric analysis revealed the same outcomes, with new bone areas of 6.41 and 2.97 mm2 in the experimental and control groups, respectively(P<0.001), and bone-to-implant contact ratios of 22.6% and 5.2%, respectively (P<0.001).

Conclusions

Using a bone patch to support the elevated sinus membrane could facilitate considerable bone regeneration from the basal bone with reduced consumption of biomaterial while simplifying the sinus augmentation procedure. The addition of rhBMP-2 could facilitate early bone regeneration around implants that are placed simultaneously.

Key Words: animal study, bone morphogenetic protein-2, bone regeneration, collagen, dental implant, maxillary sinus

De novo bone formation underneath the sinus membrane supported by a bone patch: a pilot experiment in rabbit sinus model

So-Ra Yoon

Department of Dentistry

The Graduate School, Yonsei University

(Directed by Professor Ui-Won Jung, D.D.S., M.S.D., PhD.)

Ⅰ. INTRODUCTION

Maxillary sinus provides anatomical merits for bone augmentation. After properly performed sinus augmentation (SA) procedure, the grafted biomaterial is totally surrounded by bone walls and sinus membrane (SM) containing periosteum, and thus can be stabilized without external load during the healing phase.

SA may be a challenging procedure to perform, but the contained environment for the graft material within the sinus may provide a favorable outcome. After a correctly performed SA procedure, the location of grafted

biomaterial can be well restrained by bone walls and the SM, and thus can be stabilized without the aid of a fixation device during the healing phase. Osteogenic potential is mainly provided by the surrounding bony walls, but previous studies demonstrated that SM manifested osteogenic potential under certain stimuli (Y. Choi et al. 2012; J. S. Kim et al. 2014). Thus, a dual supply of osteoprogenitor cells, not only from bony walls but also from the elevated SM, could be expected for de novo bone formation in SA (Srouji et al. 2009; Y. Choi et al. 2013).

Considering such a favorable anatomical environment, proponents of graft-free SA have claimed that maintenance of a blood clot alone under the elevated SM could be sufficient to obtain bone regeneration for supporting implants (S. H. Choi et al. 2002; Leblebicioglu et al. 2005; Hatano et al. 2007). A graft-free SA may be advantageous in decreasing biomaterial-related complications such as infection, and also the surgical time and cost (Lynch et al. 1989; Miyazono & Takaku 1989; Pierce et al. 1991). Moreover, the tissue composition of bone regenerated by graft-free SA would be similar to that of the native bone.

However, other studies have suggested that sustained air pressure and the gravity force acting on the maxillary SM may compromise the dimensional stability, which would gradually lead to the implants bulging or protruding into the internal maxillary sinus (H. R. Kim et al. 2010; Y. Choi et al. 2012). A

collagen membrane reinforced by hydroxyapatite powder has been introduced to support the elevated SM without bone grafting (Jung et al. 2015). Using the collagen membrane alone resulted in substantial bone formation around the protruded implant apex. However, further reduction of the augmented bone was found by repneumatization at the later healing phase.

Therefore, improvement of mechanical stability is required to support the elevated SM, and to maintain the regenerated bone volume for a long-term period. In order to meet this purpose, a bone patch, a combination of the mass of the bone substitute particles and the collagen membrane, has been newly devised. The bone mass adhered to the collagen membrane is expected to not only enhance the mechanical strength but also provide clinical easiness of manipulation. The bone patch can also be utilized as a carrier system for growth factors that will accelerate de novo bone formation. Since recombinant human bone morphogenetic protein-2 (rhBMP-2) has been demonstrated to stimulate the osteogenic potential of the SM (Chen et al. 2004; Li et al. 2005; J. S. Kim et al. 2014, 2015), loading rhBMP-2 on the bone patch may be beneficial to the SA procedure.

The objectives of this study were to evaluate bone regeneration beneath the bone patch lying over a concomitantly placed mini-implant following sinus floor elevation, and verify its usefulness as a carrier system for rhBMP-2 in rabbits.

Ⅱ. MATERIALS & METHODS

2.1. Animals

Five male New Zealand white rabbits weighing 2.5–3.2 kg were used. The animals were bred in separate cages under standard laboratory conditions, with ad libitum access to water and a standard laboratory pellet diet. Animal selection and care, the surgical protocol, and the preparation procedures were certified by the Institutional Animal Care and Use Committee, Yonsei Medical Center, Seoul, Korea (approval no. 2013-0335).

2.2. Experimental materials

Bone patch

Type I atelocollagen (Dalim Tissen, Seoul, Korea) was mixed with Bio-Oss® (0.25–1 mm; Geistlich Biomaterials, Wolhusen, Switzerland) and distilled water (Fig. 1). The Bio-Oss® : collagen: distilled water weight ratio was 40: 10: 1. The collagen–Bio-Oss® mixtures were poured into a PET mold, frozen at -40℃ and then lyophilized at -10℃ for 24 h. The bone block had the shape of a hexahedron, with a width of 5 mm, a length of 6 mm and a height of 2 mm. The mean weight of the bone block was 0.045g. The bilayer collagen

membrane comprised a collagen film layer and a collagen porous membrane layer. To produce the collagen film layer, type I atelocollagen was dissolved in 0.5 M acetic acid and 60 ml of the 0.8% collagen solution was poured into a petri dish and air-dried on a clean bench for 24 h. To produce the collagen porous membrane, type I atelocollagen was dispersed in distilled water, and 40 ml of the 2% collagen solution was poured into a Petri dish (12 cm × 12 cm), frozen at -40℃ and then lyophilized at -10℃ for 24 h. The bilayer membrane was produced by loading the collagen porous membrane onto the wet surface of the cross-linked collagen film. The collagen film–collagen porous membrane composite was slightly pressured and air dried, and then cut to a width of 9 mm and a length of 12 mm. Bone block was attached to the porous membrane side of the bilayer collagen membrane using collagen solution and then air-dried. The whole bone patches were cross-linked by heat dehydration in the vacuum oven at 110℃ for 24 h.

Mini-implant

The experiments used ten mini-implants with a roughened surface and dimensions of 4 mm × 3 mm (Dentium, Seoul, Korea).

RhBMP-2

The lyophilized rhBMP-2 used in this study was manufactured by the research institute of Cowellmedi (Busan, Korea), as described previously (Lee et al. 2010), at a concentration of 0.05 mg/ml.

2.3. Study design

Ten maxillary sinuses in five rabbits were used for SA. Mini-implants were placed bilaterally on the lateral wall of the maxillary sinuses following the sinus floor elevation procedure. To produce the control and experimental groups, a mini-implant and bone patch without any treatment were placed into one maxillary sinus in each animal for the control group, while a bone patch that had been soaked in rhBMP-2 was placed on the opposite side for the experimental group. The control and experimental groups were allocated alternately on the left and right sides, and a 4-week healing period was allowed.

2.4. Surgical procedure

The surgical preparation for SA and implant placement followed that used in a previous study (Y. Choi et al. 2012). The nasal dorsum of each of the five rabbits was shaved after applying general anesthesia by the intramuscular injection of a mixture of xylazine hydrochloride (Rompun, Bayer, Korea) and ketamine hydrochloride (Ketalar, Yuhan, Korea). The surgical field was disinfected with iodine solution, and then infiltration anesthesia using 2% lidocaine was applied at the nasal dorsum. An incision was made on the skin along the midline of the nasal bone to expose its dorsal surface. Two circular windows with a diameter of 5.5 mm were prepared in both sides of the nasal bone using a trephine bur (Fig. 2). The sinus mucosa was carefully elevated, and the implant sites were prepared 3 mm in front of the windows using a round bur drill and a twist drill. Before placing the mini-implants, the bone patches were inserted into their respective sinuses on the elevated SM. Two mini-implants were then placed using hand force only at each site until their shoulders were seated in the bone. The apex of mini-implant was finally in contact with the center of the bone mass. The periosteum and skin were sutured by layering with absorbable monofilament (4-0 Monosyn, B. Braun, Aesculap, PA, USA). The animals were carefully monitored during the 4-week healing period for adverse reactions around the surgical site, with

antibiotics and analgesics administered for the first 7 days. The animals were euthanized 4 weeks postoperatively using an overdose of anesthesia.

2.5. Micro-computed tomography analysis

All specimens were fixed in 10% formalin for 10 days and then scanned using a high resolution (8.88 μm) micro-computed tomography (μCT) system. μCT (SkyScan 1173, Skyscan, Kontich, Belgium) was used to evaluate three-dimensional views of bone remodeling in the harvested bone section. Digital micro radiographic images were acquired at 130 kVp and 60 μA using a 1.0-mm-thick aluminum filter. The animal was exposed to radiation for 500 ms after each 0.2-degree rotation. The pixel size was 14.91 μm. The volume of interest was limited to 4 mm in the vertical direction and 10 mm in the medial–distal direction to evaluate only the grafted bone. The following volumetric parameters (in millimeters cubed) were measured from a surface generated using a triangle meshing technique based on the marching cubes method (Bouxsein et al. 2010): total augmented volume (TV) and mineralized bone volume (MBV).

2.6. Histologic analysis

After μCT scanning, the specimens were dehydrated and embedded in methylmethacrylate resin in a vacuum chamber system. Each block was cut using a diamond cutter (Exakt, Apparatebau, Norderstedt, Germany), and sections were sawed in an anterior–posterior direction to a thickness of approximately 100 μm. These sections were then ground and polished on a diamond grinder to a thickness of 15 μm, mounted on microscope slides and stained with Masson's trichrome. The specimens were examined under a microscope (BX50, Olympus, Tokyo, Japan) equipped with a camera. The acquired images of the slides were saved as digital files. Histometric measurements were performed using automated image analysis software (Image-Pro Plus, Media Cybernetics, Silver Spring, MD, USA). The following linear parameters were measured on the stained slides by a single experienced researcher (S.R.Y.) (Jung et al. 2015): augmented height (AH), protruded height (PH), cortical bone thickness (CBT), osseointegrated height (OH), non-osseointegrated height (NOH), new bone height (NBH) (Fig. 3) and bone-to-implant contact ratio (BIC). The areal parameters of the new bone area (NBA) and remaining bone particles area (RBA) were also measured.

2.7. Statistical analysis

The median, minimum and maximum values of radiographic and histometric parameters were calculated in all groups. The significance of differences between the groups was determined using nonparametric mixed models (Brunner & Langer 2000) with the R software (version 3.1.1, http://www.r-project.org) and SPSS (version 22, IBM, Armonk, NY, USA). The cutoff for statistical significance was set at $P < 0.05$.

Ⅲ. RESULTS

3.1. Clinical observations

During the surgery, minor perforations of the SM (<1 mm) occurred at one site in the control group and at one site in the experimental group. Clinical healing was uneventful except in one animal that discharged pus, which was treated with saline irrigation and by administering antibiotics. Neither penetration of the mini-implant nor exposure of the bone patch out of the SM was detected. There was no noticeable difference in histologic, Histomorphometric and radiographic analyses.

3.2. Radiographic analysis: μCT

In cross-sectional views, de novo bone formation was evident in cross-sectional views, and radiopaque graft particles and newly formed bone were observed around mini-implant in both the control and experimental groups (Fig. 4). However, the pattern of bone formation was not consistent. The mass of new bone and residual graft material was not evenly distributed among each spatial section (medial and lateral areas). Dislocation of the bone patch to one side was more frequent in the experimental group (except in animal d in Fig. 4) compared to the control group. The radiopaque mineralized bone was

generally distributed into the lateral and anterior areas rather than into the medial and posterior areas (Fig. 5). The median values of TV and MBV were significantly higher in the experimental group than in the control group (161 vs. 122.4 mm^3 [$P < 0.01$] and 48.2 vs. 41.7 mm^3 [$P < 0.05$], respectively; Table 1).

3.3. Histologic findings and histomorphometric analysis

No inflammatory response was observed at any of the surgical sites. All mini-implants exhibited osseointegration with the original cortical bone layer and the newly formed bone tissue. The SM was in contact with the bone particles and newly formed bone. The implant apex partially protruded outside of the SM in three specimens of the experimental group, while implant apex was completely surrounded by newly formed bone and bone particles in seven specimens. Neither inflammatory responses nor adverse foreign body reactions were found irrespective of the presence of protrusion of the implant apex. No remaining collagen membrane of the bone patch was observed histologically in either group. The remaining particles were not distributed evenly: They were located anteriorly to the implant in the experimental group, and a cluster of bone substitute particles was located around the apex of the mini-implant in the control group. Most of the newly formed bone sprouted

from the basal cortical bone and grew along the implant surface to form a triangular shape. However, new bone in direct contact with bone substitute particles was rarely observed in the control group, and there was a gap between new bone and the bone patch layer (Fig. 6). In contrast, new bone grew to the SM in tight contact with the implant surface and formed a bridge with the remaining graft particles in the experimental group (Fig. 7).

The histomorphometric results are presented in Tables 2 and 3. The linear measurements of CBT, AH and NBH did not differ significantly between the two groups, whereas there were differences on the anterior side of the implant for OH (2.82 vs. 2.02 mm for the experimental and control groups, respectively; $P < 0.001$) and NOH (0.82 vs. 1.68 mm for the experimental and control groups; $P < 0.001$) (Table 2), and BIC was significantly higher in the experimental group than in the control group (22.58%and 5.21%, respectively; $P < 0.0001$).

The areal measurements of NBA and RBA differed significantly between the experimental and control groups (6.41 vs. 2.97 mm^2 [$P < 0.001$] and 1.44 vs. 4.65 mm^2 [$P < 0.01$], respectively; Table 3).

Ⅳ. DISCUSSION

The use of slow resorbing bone substitute in SA may be advantageous for pace maintenance as greater protection against pneumatization may be provided. However, if a non-vital bone substitute occupies the grafted site, this might reduce the space for angiogenesis and migration of osteogenic progenitor cells, which might in turn limit the formation of new bone (Laurencin et al. 2006). Therefore, maintenance of the elevated SM for blood coagulum stabilization is the first priority for an implant placed with a simultaneous SA. In the present study, we developed a bone patch for securing space under the elevated SM.

The approach adopted in the present study was similar to Jung et al. (2015) using a collagen membrane reinforced by hydroxyapatite powder for space maintenance under the elevated SM in rabbits, except that a bone patch was used in the present study. That previous approach resulted in substantial de novo bone formation beneath the collagen membrane; however, the augmented volume was extensively reduced at 8 weeks, which was attributable to poor mechanical stability. Repneumatization was avoided in the present study by attaching bone substitute to the membrane so as to provide mechanical strengthening. As expected, this approach was effective at supporting the elevated SM in situ, with no collapse in the space created

around the implant where the natural provisional matrix would form. The results of the present study clearly indicate that the use of a bone patch met our presurgical expectations, in that the bone patch could support the elevated SM, analogously to an umbrella. However, further study is needed to confirm the dimensional stability against repneumatization at a later time point.

A particularly interesting observation was of a substantial amount of bone regeneration around the implant irrespective of whether rhBMP-2 was present on the bone patch. The implant protruded approximately 3.4 mm into the sinus cavity after installation, with 2.8 and 2.0 mm of bone apposition anteriorly along the implant surface (i.e., OH) in the experimental and control groups, respectively, which are equivalent to 78% and 55% of the exposed implant length in the sinus cavity, respectively. As the elevated SM did not collapse (AH > PH), the NOH could have subsequently reduced.

The linear measurements made on the anterior and posterior sides of the implant revealed differences in the healing pattern, with the measured values tending to be higher on the anterior side. This difference might be associated with the vicinity of the axial bone wall in the anterior compartment, which would provide a favorable environment for wound stability and bone regeneration with air pressure within the sinus (Asai et al. 2002; Xu et al. 2005). Furthermore, this side difference might also be affected by dislocation of the bone patch, especially in the rhBMP-2 group during the healing phase.

The bone patches were in contact with the implant apex without rigid fixation in both groups at the end of the surgery, but the bone patches in the experimental group in particular were noticeably displaced at the time of death. Swelling by a chemotax is effect of rhBMP-2 at the early stage of healing was attributable to the movement (Smucker et al. 2006).

Dislocation of bone patch might be associated with its size. A suitable size for the bone patch could not be accurately predicted, as the current pilot study was the first attempt at using such a device. For the clinical usage, the bone patch would be constructed at a sufficient size to avoid dislocation. Furthermore, the lack of direct contact between new bone and the biomaterials might be attributable to the early healing time. In the present study, observations were made after 4 weeks of healing, which might be too early for substantial bone formation. On the other hand, as BMP-2 can accelerate bone formation, considerable bone formation and direct contact could be observed compared to the control group. The possibility of denaturation of the bone substitute during adhesion to the collagen membrane cannot be excluded.

The bone regenerative effects as revealed by the volumetric and areal analyses were greater in the experimental group than in the control group, with different bone growth patterns. Direct contact of the bone patch and newly formed bone was hardly found in the control group, whereas active ingrowth of new bone into the bone patch and tight interconnection between the bone

substitute and new bone were found in the experimental group. However, the present result should be interpreted conservatively due to the limited sample size, 10 sites in five animals.

Osteogenic stimulation of rhBMP-2 to the overlying SM is of considerable interest in SA, because it can lead multidirectional bone formation (Kubler et al. 1998; Bessho et al. 2000; Vallejo et al. 2002; Long et al. 2006). We previously demonstrated acceleration of ossification near the SM in an rhBMP-2 group (Y. Choi et al. 2013; M. S. Kim et al. 2014b). When a high dose of rhBMP-2 (1.5 mg/ml) was used, the total amount of new bone was significantly decreased compared to the control, whereas bone formation near the SM showed a statistically significant increase (Y. Choi et al. 2013). When a low dose of rhBMP-2 (0.15 mg/ml) was applied, new bone in the area adjoining the SM appeared to increase (M. S. Kim et al. 2014b). In line with these previous studies, the present study also found that rhBMP-2 facilitated new bone formation on the SM in the experimental group within 4 weeks in a rabbit model and that rhBMP-2 could be easily applied using the bone patch as a carrier. In clinical situations, the bone patch can shorten the SA procedure by simplifying a graft procedure. Moreover, the addition of rhBMP-2 may shorten the healing time of multidirectional bone regeneration toward the implant.

Ⅴ. CONCLUSION

The newly devised bone patch in this study can support the elevated SM and facilitate bone regeneration from the basal bone with a reduced amount of biomaterial. In clinical applications the bone patch can simplify the SA procedure by avoiding the need for a grafting procedure. Moreover, the addition of rhBMP-2 may shorten the healing time for multidirectional bone regeneration towards the implant. However, further studies with increased sample size and the other experimental models should be needed to apply the present result to clinical practice as an effective and convenient protocol.

REFERENCES

Asai, S., Shimizu, Y. & Ooya, K. (2002) Maxillary sinus augmentation model in rabbits: effect of occluded nasal ostium on new bone formation. Clinical Oral Implants Research 13: 405-409.

Bessho, K., Konishi, Y., Kaihara, S., Fujimura, K., Okubo, Y. & Iizuka, T. (2000) Bone induction by Escherichia coli -derived recombinant human bone morphogenetic protein-2 compared with Chinese hamster ovary cell-derived recombinant human bone morphogenetic protein-2. The British Journal of Oral & Maxillofacial Surgery 38: 645-649.

Bouxsein, M.L., Boyd, S.K., Christiansen, B.A., Guldberg, R.E., Jepsen, K.J. & Muller, R. (2010) Guidelines for assessment of bone microstructure in rodents using micro-computed tomography. Journal of Bone and Mineral Research 25: 1468-1486.

Chen, D., Zhao, M. & Mundy, G.R. (2004) Bone morphogenetic proteins. Growth Factors (Chur, Switzerland) 22: 233-241.

Choi, S.H., Kim, C.K., Cho, K.S., Huh, J.S., Sorensen, R.G., Wozney, J.M. & Wikesjo, U.M. (2002) Effect of recombinant human bone morphogenetic protein-2/absorbable collagen sponge (rhBMP-2/ACS) on healing in 3-wall intrabony defects in dogs. Journal of Periodontology 73: 63-72.

Choi, Y., Lee, J.S., Kim, Y.J., Kim, M.S., Choi, S.H., Cho, K.S. & Jung, U.W. (2013) Recombinant human bone morphogenetic protein-2 stimulates the osteogenic potential of the Schneiderian membrane: a histometric analysis in rabbits. Tissue Engineering. Part A 19: 1994-2004.

Choi, Y., Yun, J.H., Kim, C.S., Choi, S.H., Chai, J.K. & Jung, U.W. (2012) Sinus augmentation using absorbable collagen sponge loaded with Escherichia coli-expressed recombinant human bone morphogenetic protein 2 in a standardized rabbit sinus model: a radiographic and histologic analysis. Clinical Oral Implants Research 23: 682-689.

Hatano, N., Sennerby, L. & Lundgren, S. (2007) Maxillary sinus augmentation using sinus membrane elevation and peripheral venous blood for implant-supported rehabilitation of the atrophic posterior maxilla: case series. Clinical Implant Dentistry and Related Research 9: 150-155.

Jung, U.W., Unursaikhan, O., Park, J.Y., Lee, J.S., Otgonbold, J. & Choi, S.H. (2015) Tenting effect of the elevated sinus membrane over an implant with adjunctive use of a hydroxyapatite-powdered collagen membrane in rabbits. Clinical Oral Implants Research 26: 663-670.

Kim, H.R., Choi, B.H., Xuan, F. & Jeong, S.M. (2010) The use of autologous venous blood for maxillary sinus floor augmentation in conjunction with sinus membrane elevation: an experimental study. Clinical Oral Implants Research 21: 346-349.

Kim, J.S., Cha, J.K., Cho, A.R., Kim, M.S., Lee, J.S., Hong, J.Y., Choi, S.H. & Jung, U.W. (2014) Acceleration of Bone Regeneration by BMP-2-Loaded Collagenated Biphasic Calcium Phosphate in Rabbit Sinus. Clinical Implant Dentistry and Related Research.

Kim, J.S., Cha, J.K., Cho, A.R., Kim, M.S., Lee, J.S., Hong, J.Y., Choi, S.H. & Jung, U.W. (2015) Acceleration of Bone Regeneration by BMP-2-Loaded Collagenated Biphasic Calcium Phosphate in Rabbit Sinus. Clinical Implant Dentistry and Related Research 17: 1103-1113.

Kim, M.S., Kwon, J.Y., Lee, J.S., Song, J.S., Choi, S.H. & Jung, U.W. (2014) Low-dose recombinant human bone morphogenetic protein-2 to enhance the osteogenic potential of the Schneiderian membrane in the early healing phase: in vitro and in vivo studies. Journal of Oral and Maxillofacial Surgery 72: 1480-1494.

Kubler, N.R., Reuther, J.F., Faller, G., Kirchner, T., Ruppert, R. & Sebald, W. (1998) Inductive properties of recombinant human BMP-2 produced in a bacterial expression system. International Journal of Oral and Maxillofacial Surgery 27: 305-309.

Laurencin, C., Khan, Y. & El-Amin, S.F. (2006) Bone graft substitutes. Expert Review of Medical Devices 3: 49-57.

Leblebicioglu, B., Ersanli, S., Karabuda, C., Tosun, T. & Gokdeniz, H. (2005) Radiographic evaluation of dental implants placed using an osteotome technique. Journal of Periodontology 76: 385-390.

Lee, J.H., Kim, C.S., Choi, K.H., Jung, U.W., Yun, J.H., Choi, S.H. & Cho, K.S. (2010) The induction of bone formation in rat calvarial defects and subcutaneous tissues by recombinant human BMP-2, produced in Escherichia coli. Biomaterials 31: 3512-3519.

Li, G., Cui, Y., McIlmurray, L., Allen, W.E. & Wang, H. (2005) rhBMP-2, rhVEGF(165), rhPTN and thrombin-related peptide, TP508 induce chemotaxis of human osteoblasts and microvascular endothelial cells. Journal of Orthopaedic Research 23: 680-685.

Long, S., Truong, L., Bennett, K., Phillips, A., Wong-Staal, F. & Ma, H. (2006) Expression, purification, and renaturation of bone morphogenetic protein-2 from Escherichia coli. Protein Expression and Purification 46: 374-378.

Lynch, S.E., Colvin, R.B. & Antoniades, H.N. (1989) Growth factors in wound healing. Single and synergistic effects on partial thickness porcine skin wounds. The Journal of Clinical Investigation 84: 640-646.

Miyazono, K. & Takaku, F. (1989) Platelet-derived growth factors. Blood Reviews 3: 269-276.

Pierce, G.F., Mustoe, T.A., Altrock, B.W., Deuel, T.F. & Thomason, A. (1991) Role of platelet-derived growth factor in wound healing. Journal of Cellular Biochemistry 45: 319-326.

Smucker, J.D., Rhee, J.M., Singh, K., Yoon, S.T. & Heller, J.G. (2006) Increased swelling complications associated with off-label usage of rhBMP-2 in the anterior cervical spine. Spine (Phila Pa 1976) 31: 2813-2819.

Srouji, S., Kizhner, T., Ben David, D., Riminucci, M., Bianco, P. & Livne, E. (2009) The Schneiderian membrane contains osteoprogenitor cells: in vivo and in vitro study. Calcified Tissue International 84: 138-145.

Vallejo, L.F., Brokelmann, M., Marten, S., Trappe, S., Cabrera-Crespo, J., Hoffmann, A., Gross, G., Weich, H.A. & Rinas, U. (2002) Renaturation and purification of bone morphogenetic protein-2 produced as inclusion bodies in high-cell-density cultures of recombinant Escherichia coli. Journal of Biotechnology 94: 185-194.

Xu, H., Shimizu, Y. & Ooya, K. (2005) Histomorphometric study of the stability of newly formed bone after elevation of the floor of the maxillary sinus. The British Journal of Oral & Maxillofacial Surgery 43: 493-499.

FIGURES

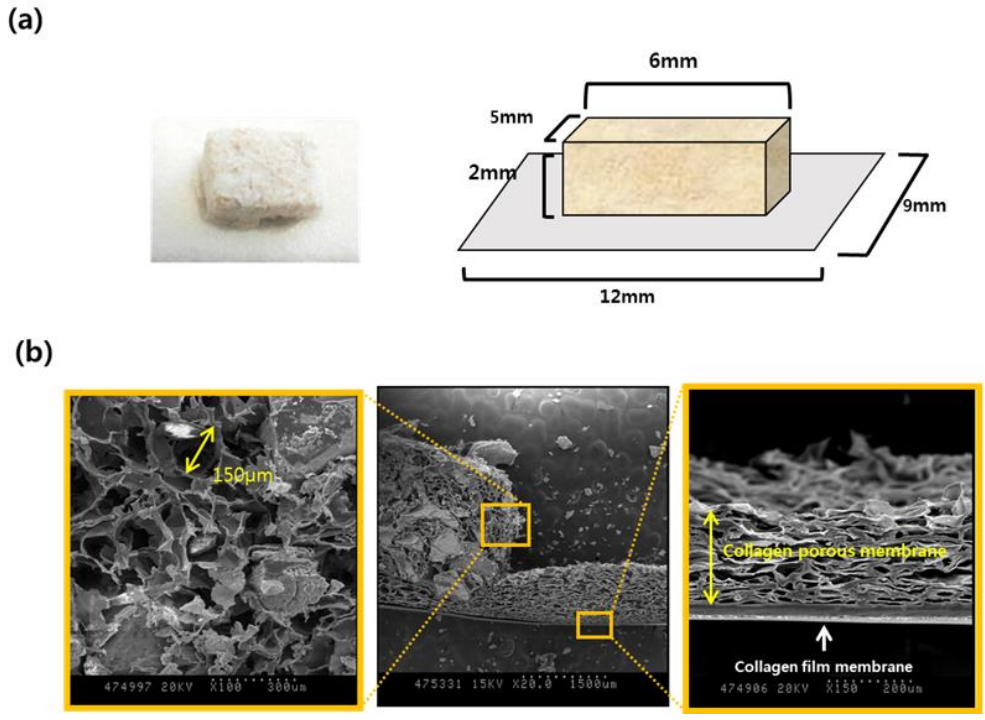

Figure 1. Clinical photograph and simplified diagram and Scanning electron microscopy.

(a) Clinical photograph and simplified diagram of the newly devised bone substitute combined with collagen membrane (called a bone patch). (b) Scanning electron microscopy of the one patch showed a mixture of bone substitute particles and collagen fiber network attached to the collagen membrane, which comprised film and porous layers of collagen.

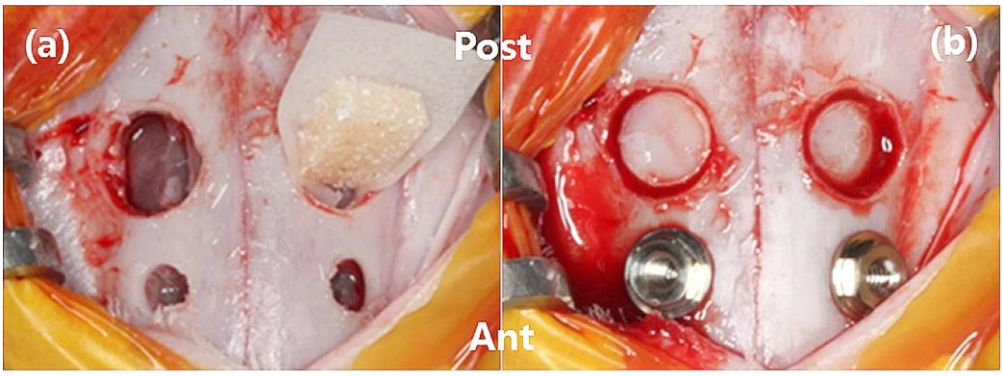

Figure 2. Representative clinical photographs of the surgical procedures.

(a) Two symmetric, circular osteotomies with a diameter of 5.5 mm were produced surgically, and another two osteotomies were performed to allow placement of the dental implants. The sinus membrane (SM) was elevated and the newly devised bone patch was inserted into the locations of dental implants via the 5.5-mm-diameter bony windows. At test sites, the bone patch was installed after soaking it in recombinant human bone morphogenetic protein-2 (rhBMP-2). (b) After installing the dental implants, the circular bony fragments were replaced into their original positions.

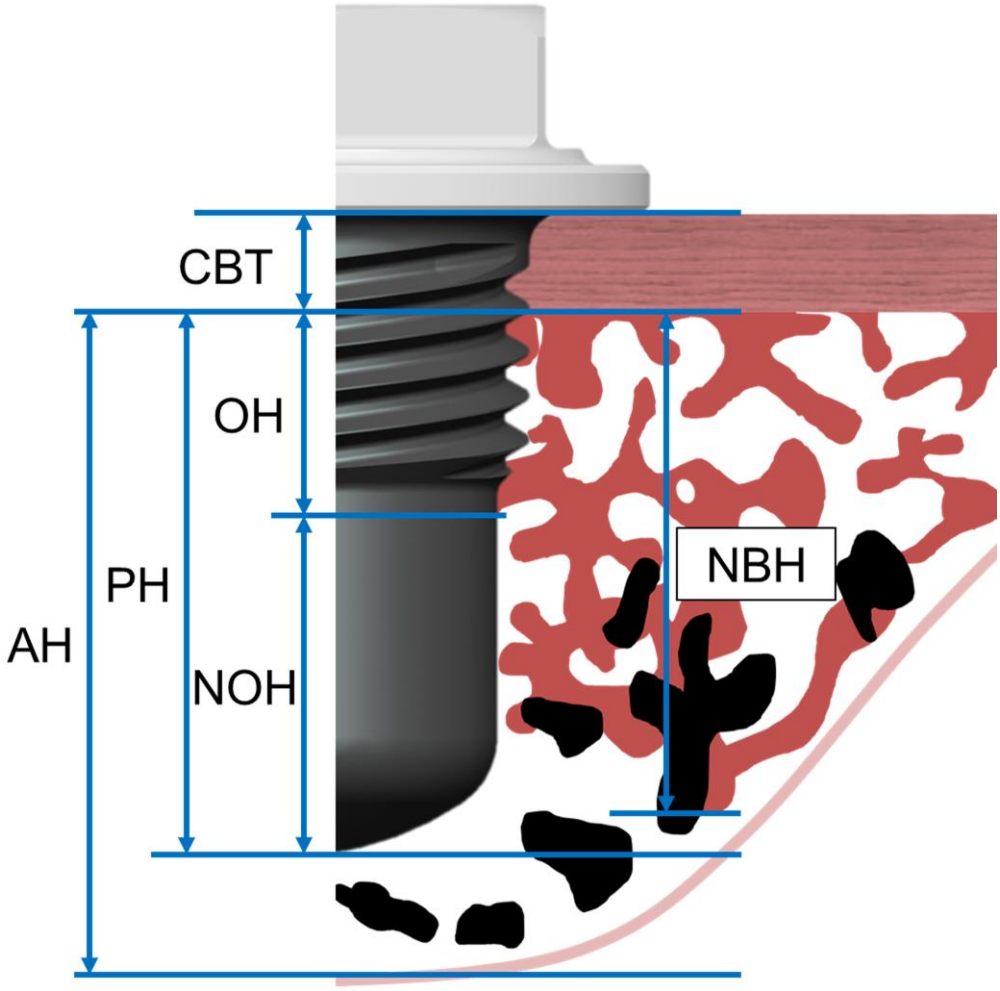

Figure 3. Diagram of the following linear measurements made on histologic slides:

Augmented height (AH), protruded height (PH), cortical bone thickness (CBT), osseointegrated height (OH), non-osseointegrated height (NOH) and new bone height (NBH).

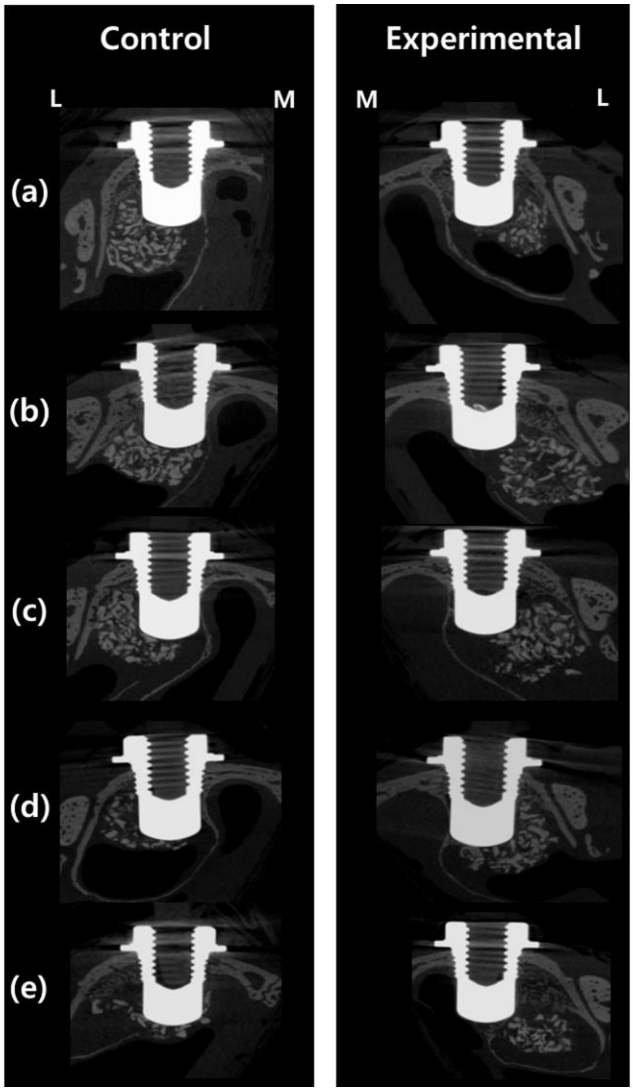

Figure 4. Cross-sectional views of micro-computed tomography (μCT) in all control and experimental samples (M: medial, L: lateral).

All sites showed grafted biomaterials within the spaces between the intruded dental implants and the sinus membrane.

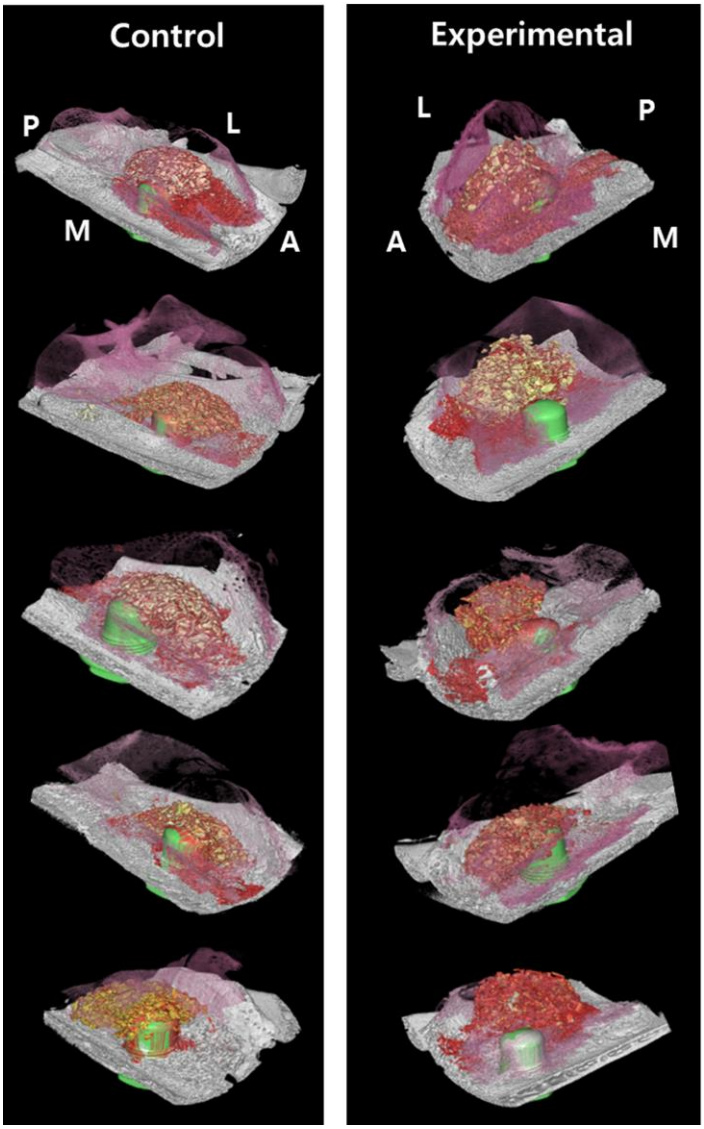

Figure 5. Three-dimensionally reconstructed images of all control and experimental samples

Residual biomaterials (yellow), newly formed bone (red) and dental implants (green) are coded with different colors on all of the cross-sectional images and reconstructions (M: medial, L: lateral, A: anterior, P: posterior).

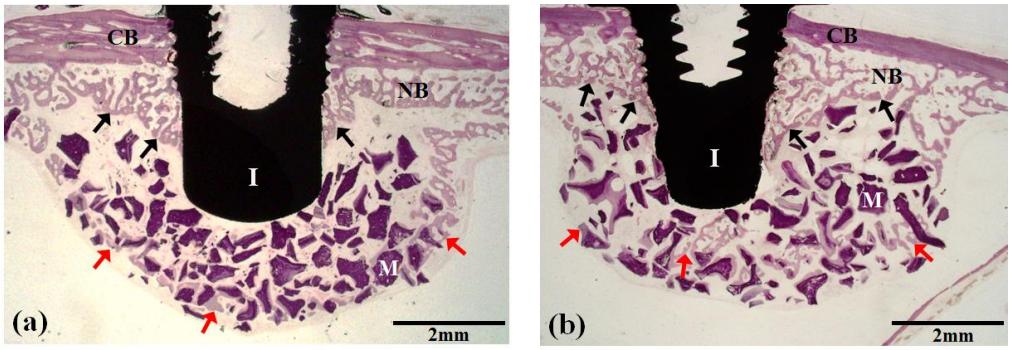

Figure 6. Representative photomicrographs of control and experimental sites.

Representative photomicrographs of control (a) and experimental (b) sites. Newly formed bone (NB) and residual biomaterials (M) were observed around the intruded dental implants (I) at experimental sites, while the control sites showed minimal bone formation within the grafted area with bone substitutes. Newly formed bone sprouted from the basal bone (black arrows) and from the elevated Schneiderian membrane (red arrows). (CB, cortical bone).

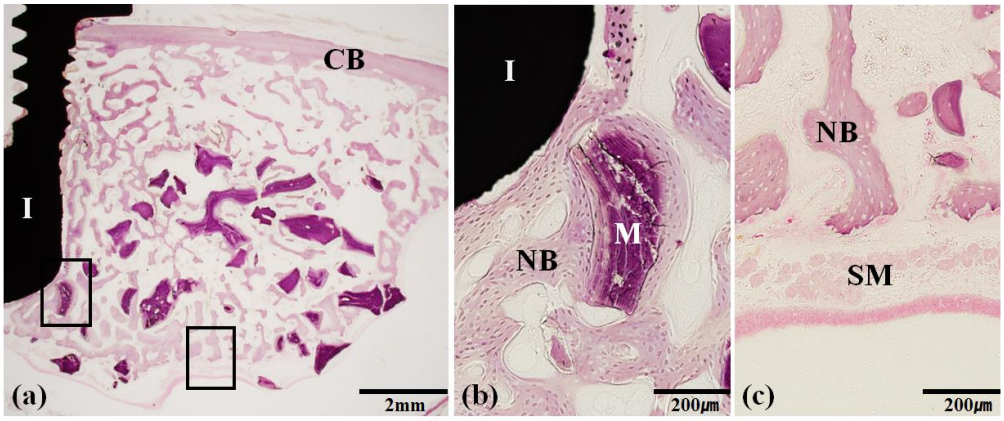

Figure 7. Histologic views of the experimental sites showing dislocation of the bone patch.

(a) Histologic views of the experimental sites showing dislocation of the bone patch.

(b) New bone formation was found along the entire length of dental implant (I) surface, directly contacting the residual biomaterials (M).

(c)Higher magnified view at the elevated Schneiderian membrane (SM)(CB, cortical bone).

TABLES

Table 1. Volumetric analysis in micro-computed tomography (n = 5; medians [min, max]; mm^3).

	Experimental	Control	*P*-value
TV	161.0* [132.3, 228.0]	122.4 [113.0, 178.4]	0.003
MBV	48.2* [36.6, 79.6]	41.7 [26.7, 47.6]	0.047
STV	112.8 [87.0, 158.5]	81.6 [74.4, 130.8]	0.067

*Significantly higher than control group ($P < 0.05$).

Table 2. Linear histometric analysis (n = 5; medians [min, max]; mm).

		Experimental	Control	*P*-value
NBH	Anterior	4.45 [3.88, 5.49]	3.82 [2.24, 4.47]	0.07
	Posterior	2.42 [1.99, 4.56]	3.04 [1.42, 4.67]	0.92
CBT	Anterior	0.25 [0.38, 0.20]	0.3 [0.35, 0.21]	0.87
	Posterior	0.29 [0.39, 0.19]	0.3 [0.36, 0.25]	0.49
OH	Anterior	2.82* [378, 2.28]	2.02 [2.64, 1.38]	0.000008
	Posterior	2.66 [3.65, 2.24]	1.46 [3.40, 1.38]	0.13
NOH	Anterior	0.82* [1.46, 0.00]	1.68 [2.29, 1.15]	0.0001
	Posterior	1.04 [1.57, 0.00]	0.24 [2.74, 0.30]	0.24
AH		5.05 [4.45, 5.74]	5.07 [4.35, 5.97]	0.89

*Significantly higher than control group ($P < 0.01$).

Table 3. Planimetric histometric analysis (n = 5; medians [min, max]; mm^2).

	Experimental	Control	*P*-value
TA	29.69 [23.50, 35.54]	26.05 [18.85, 37.17]	0.487
NBA	6.41* [1.34, 11.02]	2.97 [1.28, 3.60]	0.0005
RBA	1.44* [0.31, 4.39]	4.65 [3.62, 7.05]	0.0022
STA	23.94 [19.0, 25.22]	17.23 [13.95, 29.64]	0.3018

*Significantly higher than control group ($P < 0.01$).

국문초록

토끼에서 Bone patch 를 이용한 상악동막 거상술에 관한 방사선학적, 조직계측학적 연구

< 지도교수 정 의 원 >

연세대학교 대학원 치의학과

윤 소 라

연구의 목적

호흡에 의해 상악동 막에 지속적으로 가해지는 함기화에 저항하기 위해 bone patch 라 명명된 콜라겐 차폐막/ 골 이식재 복합체가 새롭게 고안되었다. 콜라겐 차폐 막을 사용하여 상악동 거상술을 하였지만 차폐막의 수화로 인하여 계속적인 함기화에 공간 유지가 어려웠고 상악동 공간 유지를 위한 방법을 보안해 주고자 콜라젠 차폐 막에 골 이식재를 더하여 기존 콜라젠 차폐 막에 비해 기계적 강도를 높인 bone patch 를 이용하여

거상된 막의 위치를 유지함으로써 거상된 상악동 막 하방의 신생골 형성을 유도하기 위함이다.

본 연구의 목적은 토끼에서 bone patch 를 이용하여 상악동 거상술과 동시에 임플란트를 식립했을 때, 상악동내 골 재생을 평가하고, 또한 골 형성 유도단백질-2(rhBMP-2)를 위한 전달 시스템으로써 bone patch 의 유용성을 검증하기 위함이다.

연구재료 및 방법

본 연구에서는 총 5 마리의 뉴질랜드 흰 토끼를 사용하였다. 토끼의 상악동 부분에 지름 5.5mm 의 골 결손 부를 형성한 후, 상악동 막을 조심스럽게 거상했다. 상악동 막 거상을 통해 형성된 공간에, 대조군은 식염수를 적용한 bone patch 를 이식했고, 실험군은 rhBMP-2 를 적용한 bone patch 를 이식하였다. 골 창 앞부분에 드릴링 후, 4mm × 3mm 의 미니 임플란트를 식립하였다. 실험군 과 대조군은 무작위로 군 설정을 하였고, 4 주 후에 5 마리 모두 희생하여 조직을 적출했다. 마이크로 전산화 단층 촬영과 조직학적 및 조직계측 학적 분석을 시행하였다.

연구 결과

4 주 후의 방사선 및 조직계측학적 분석 결과, 미니 임플란트 주변으로 방사선 불투과성의 신생골 형성을 확인하였다. 방사선 계측 결과, 상악동 증강 부피에 있어서 전체적인 골양과 신생골에서 실험군이 대조군 보다 유의하게 더 높았다 [161 vs. 122 mm^3; 48 vs. 42 mm^3 (P<0.05)]. 조직학적 분석 결과 또한 신생골 형성에 있어서, 모든 임플란트에서 기존 골과 새로운 골의 골 유착을 보였다. 임플란트 정점 부분이 돌출한 것은 실험군에서 3 개를 제외하고는 돌출되지 않았고 기존 골에서부터 골이 생성되고 삼각형 모양을 형성하였다. 대조군에서 임플란트 표면을 따라 골 성장이 관찰되었고, 생성된 골과 본 패치 층 사이에는 간격이 관찰되었다. 그러나 대조군의 재료 입자와 직접 접촉하는 신생골은 관찰되지 않았다. 반면 실험군의 임플란트 표면을 따라 성장하여 삼각 형태의 모양을 형성하는데 신생골은 임플란트 표면과 함께 상악동 막에 새로운 신생골이 생성되었고, 연결된 형태로 신생골들이 형성되었다. 신생골 면적계측에서 실험군 6.41mm^2 과 대조군 2.97mm^2 로 실험군에서 대조군 보다 더 높았고 유의한 차이를 보였다. 골-임플란트 접촉은 실험군이 22.6%이고 대조군이 5.2%로 두 군간의 유의한 차이를 보였다($p < 0.001$).

결론

토끼 상악동 거상술 모델에서, bone patch 는 거상된 상악동 막을 지지함으로써, 상악동 막 하방에 형성된 공간에 골 재생을 유도할 수 있었고, 부가적인 골 형성 유도단백질사용을 통해 골 형성을 촉진시킬 수 있었다.

핵심되는 말 : 골형성유도 단백질 2; 골재생; 상악동; 멤브레인; 토끼 상악동 모델